Enhanced solid-state multispin metrology using dynamical decoupling

L. M. Pham,[1] N. Bar-Gill,[2,3] C. Belthangady,[2] D. Le Sage,[2] P. Cappellaro,[4] M. D. Lukin,[3] A. Yacoby,[3] and R. L. Walsworth[2,3]

[1]*School of Engineering and Applied Sciences, Harvard University, Cambridge, Massachusetts 02138, USA*

[2]*Harvard-Smithsonian Center for Astrophysics, Cambridge, Massachusetts 02138, USA*

[3]*Physics Department, Harvard University, Cambridge, Massachusetts 02138, USA*

[4]*Nuclear Science and Engineering Department, Massachusetts Institute of Technology, Cambridge, Massachusetts 02139, USA*

(Received 26 January 2012; revised manuscript received 23 May 2012; published 24 July 2012)

We use multipulse dynamical decoupling to increase the coherence lifetime (T_2) of large numbers of nitrogen-vacancy (NV) electronic spins in room temperature diamond, thus enabling scalable applications of multispin quantum information processing and metrology. We realize an order-of-magnitude extension of the NV multispin T_2 in three diamond samples with widely differing spin impurity environments. In particular, for samples with nitrogen impurity concentration $\lesssim$1 ppm, we extend T_2 to >2 ms, comparable to the longest coherence time reported for single NV centers, and demonstrate a tenfold enhancement in NV multispin sensing of ac magnetic fields.

DOI: 10.1103/PhysRevB.86.045214 PACS number(s): 03.65.Yz, 05.60.Gg, 07.55.Ge, 76.30.Mi

I. INTRODUCTION

The negatively charged nitrogen-vacancy (NV) color center in diamond possesses many useful properties—long electronic spin coherence times at room temperature, an optical mechanism for initializing and detecting the spin state, and the ability to coherently manipulate the spin using electron spin resonance (ESR) techniques—which make it a leading solid-state system for scalable applications in quantum information and metrology, such as sensitive detection of electric and magnetic fields with high spatial resolution[1–9] or in bulk.[10–12] Recently, dynamical decoupling techniques have been used to reduce the effective interaction of single NV spins with other spin impurities in the environment, specifically in impurity environments dominated either entirely by nitrogen (N) electronic spins ($\sim$100 ppm)[13,14] or entirely by ^{13}C nuclear spins,[15,16] thereby enabling significant improvements in the NV single-spin coherence lifetime (T_2)[13,15,16] and ac magnetic field sensitivity.[14,16]

In this paper we demonstrate in room temperature diamond the equally successful application of dynamical decoupling to large numbers of NV spins ($>10^3$), despite the greater inhomogeneities in local impurity environment and subsequently less optimal average control pulse fidelity as compared to addressing single NV spins. We employ multipulse Carr-Purcell-Meiboom-Gill (CPMG) and XY control sequences[17–19] to improve both the NV multispin T_2 and ac magnetic field sensitivity by an order of magnitude. Furthermore, we find similar relative improvements for diamond samples with widely differing NV densities and spin impurity concentrations, including two impurity environment regimes for which NV dynamical decoupling has not previously been demonstrated. We also show that the scaling of T_2 with the number of pulses in the control sequence depends nontrivially on the concentration of N and ^{13}C impurities, and can differ from the scaling obtained in previous single NV measurements.[13,15,16] For some samples, the NV multispin T_2 is increased to >2 ms, where it begins to be limited by NV spin-lattice relaxation ($T_1 \approx 6$ ms). These demonstrations of the utility of dynamical decoupling for solid-state multispin systems pave the way for scalable applications of quantum information processing and metrology in a wide range of architectures, including multiple NV centers in bulk diamond,[1,12,20] two-dimensional (2D) (thin-layer) arrays,[6,21–23] and diamond nanostructures[24,25]; as well as phosphorous donors in silicon[26,27] and quantum dots.[28]

The NV center is composed of a substitutional nitrogen impurity and a vacancy on adjacent lattice sites in the diamond crystal [Fig. 1(a)]. The electronic structure of the negatively charged state of the NV center has a spin-triplet ground state, where the $m_s = \pm 1$ levels are shifted from the $m_s = 0$ level by $\sim$2.87 GHz due to the dipolar spin-spin interaction [Fig. 1(b)]. Application of an external static magnetic field along the NV axis Zeeman shifts the $m_s = \pm 1$ levels and allows one to treat the $m_s = 0$, $m_s = +1$ spin manifold (for example) as an effective two-level system. The NV spin state can be initialized in the $m_s = 0$ state with above-band laser excitation, manipulated with resonant microwave (MW) pulses, and read out optically by measuring the spin-state-dependent fluorescence intensity in the phonon sideband.

II. MULTISPIN DYNAMICAL DECOUPLING

The NV spin environment (i.e., spin bath) is typically dominated by ^{13}C and N impurities, randomly distributed in the diamond crystal. These spin impurities create time-varying local magnetic fields at each NV spin, which can be approximated as an average local magnetic field that fluctuates on a time scale set by the mean interaction between spins in the bath, inducing rapid dephasing of freely precessing NV spins on a time scale $T_2^* \sim 1$ μs for typical spin impurity concentrations. By applying a single resonant MW π pulse to refocus the dephasing, the Hahn echo sequence [Fig. 1(c)] decouples NV spins from bath field fluctuations that are slow compared to the free precession time.[1,2] Application of additional control pulses, as in n-pulse CPMG (CPMG-n) and XY sequences, have recently been shown to decouple single NV spins from higher frequency bath fluctuations.[13,15,16]

In the present study we used a wide-field fluorescence microscope to perform dynamical decoupling and magnetometry measurements on large numbers of NV centers in three

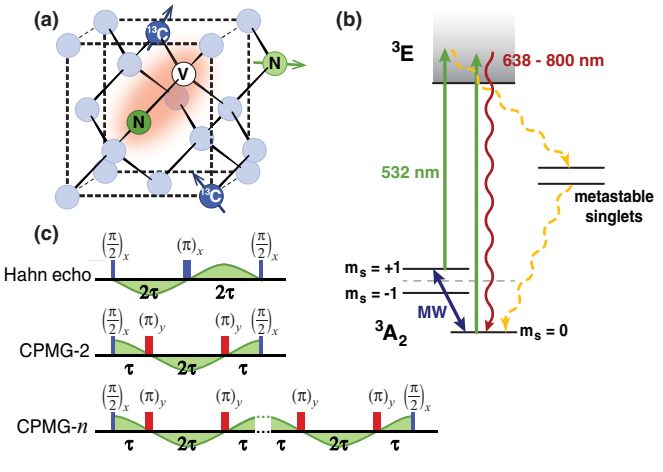

FIG. 1. (Color online) (a) Nitrogen-vacancy (NV) color center in a diamond lattice. NV electronic spin decoherence is dominated by ^{13}C nuclear spin and N electronic spin impurities. (b) Energy level structure of negatively charged NV center. (c) Hahn echo and n-pulse CPMG control sequences. Timing of ac magnetic field to be measured is shown in green.

diamond samples with very different NV densities and spin impurity environments. A switched 3 W, 532 nm laser provided optical excitation of NV centers within a 10-μm-diameter cross section of each sample. NV spin-state-dependent fluorescence was collected by a microscope objective and imaged onto a CCD array. Resonant MW control pulses for coherent manipulation of the NV spin states were applied using a loop antenna designed to generate a homogeneous B_1 field over the sample detection volume. Applying a static field ($B_0 \sim 70$ G) along one of the four diamond crystallographic axes selected approximately one quarter of the NV centers to be resonant with the MW pulses. Each diamond sample consisted of an NV-rich layer grown by chemical vapor deposition on a nonfluorescing diamond substrate, such that all collected fluorescence could be attributed to the NV-rich layer.

Sample A (Apollo) had a 16-μm-thick NV-rich layer with NV concentration ~60 ppb (measured by NV fluorescence intensity), N concentration ~100 ppm (measured by secondary ion mass spectroscopy), and 1.1% natural abundance ^{13}C concentration. The high N concentration dominated NV decoherence in this sample, limiting the measured Hahn echo multispin coherence time to $T_2 \approx 2$ μs. We applied CPMG-n sequences and determined the NV multispin coherence time as a function of the number of pulses $T_2^{(n)}$ from the $1/e$ decay of the spins' coherent evolution as a function of the total CPMG-n evolution period [Fig. 1(c)]. (As in any realistic experimental realizations, the applied pulses are of finite duration.[30]) Representative measurements of NV multispin coherence decay are shown in Fig. 2(a), with $T_2^{(n)}$ extended by a factor >10 for $n = 128$ [Fig. 2(d)]. Furthermore, we found that $T_2^{(n)}$ exhibited a power-law dependence on n: $T_2^{(n)} \propto n^s$, with $s = 0.65 \pm 0.02$ for sample A, which is consistent with the value $s \approx 0.67$ found recently for single NV centers in similarly nitrogen-rich diamond samples.[13] These results demonstrate that inhomogeneities in the spin bath and MW field do not limit the effectiveness of dynamical decoupling for extending solid-state

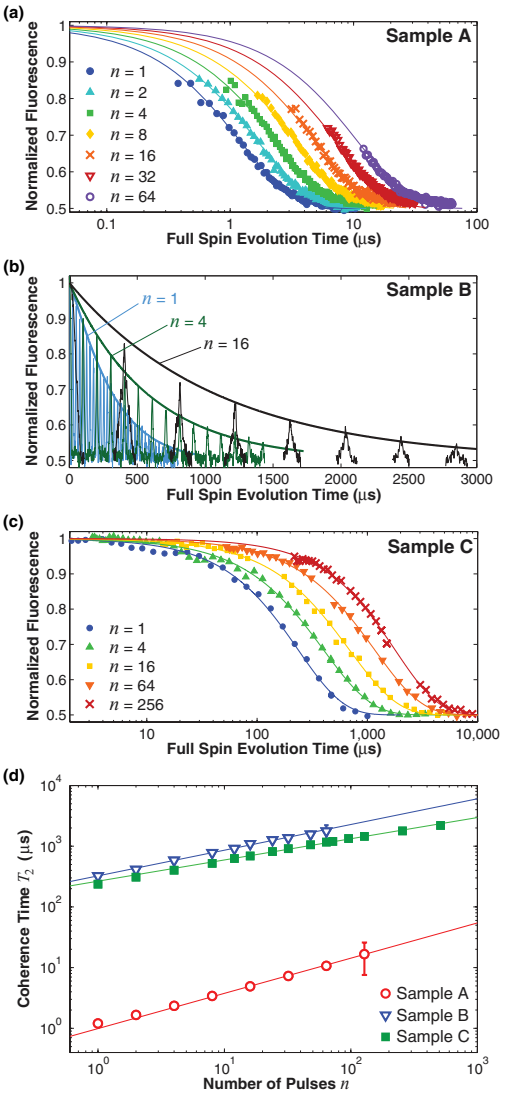

FIG. 2. (Color online) Measurements of NV multispin coherent evolution using n-pulse CPMG control sequences for three diamond samples of differing NV densities and spin impurity environments: (a) NV ~ 60 ppb, N ~ 100 ppm, and 1.1% ^{13}C; (b) NV ~ 0.2 ppb, N ~ 0.1 ppm, and 1.1% ^{13}C; and (c) NV ~ 0.6 ppb, N ~ 1 ppm, and 0.01% ^{13}C, where the solid lines denote fits to the decoherence envelope of the form $\exp[-(\tau/T_2)^p]$. Note that the time axis of (b) is plotted with a linear scale due to the periodic collapses and revivals in the NV spin coherence of sample B associated with ^{13}C Larmor precession.[29] These collapses and revivals occur in samples where the ^{13}C abundance is high enough to contribute significantly to NV decoherence. (d) Scaling of measured NV multispin coherence times with the number n of CPMG pulses: $T_2 \propto (n)^s$.

multispin coherence times by at least an order of magnitude. Note that the obtained coherence times are representative of the coherence for an arbitrary initial state since the symmetrized XY family of pulse sequences are equally effective for any coherent superposition state (and for components along the quantization axis, T_1 is longer than T_2). We demonstrate the efficacy of XY pulse sequences for an arbitrary initial state in the analysis of magnetic field sensitivity (see below).

The NV-rich layers of samples B (Apollo) and C (Element Six) had much lower NV and N concentrations than in sample A: NV ~ 0.2 ppb, N ~ 0.1 ppm for sample B and NV ~ 0.6 ppb, N ~ 1 ppm for sample C. However, sample B contained 1.1% natural abundance ^{13}C such that both N and ^{13}C contributed to NV decoherence, resulting in periodic collapses and revivals in the NV spin coherence associated with ^{13}C Larmor precession.[29] In contrast, sample C was isotopically engineered to reduce the ^{13}C concentration to 0.01% such that N impurities still dominated NV decoherence. Despite these differences in spin impurity environments, we measured similar Hahn echo NV multispin coherence times ($T_2 \sim 300\ \mu$s) for the two samples. By applying n-pulse CPMG dynamical decoupling sequences, we extended the multispin $T_2^{(n)}$ to ≈ 2 ms for both samples [Figs. 2(b) and 2(c)], which is comparable to the longest coherence time reported for dynamical decoupling applied to single NV centers.[16] At these long coherence times, the contribution of T_1 processes to decoherence (through the relation $T_2^{(\max)} \sim T_1$[31]) begins to be measurable (see Ref. 30 and also see similar effects in single NV measurements in Ref. 16).

Note that the spin impurity environments of samples B and C differ significantly from any diamond samples previously studied with NV dynamical decoupling. For these samples we observed a power-law dependence for $T_2^{(n)} \propto n^s$ [Fig. 2(d)], with lower scaling powers than for the N-rich sample A: $s = 0.42 \pm 0.02$ for sample B and $s = 0.35 \pm 0.01$ for sample C. These sample-dependent scaling powers, and the demonstration of similar behavior for NV single-spin and NV multispin decoherence in samples with comparable impurity environments, suggest that multipulse dynamical decoupling control sequences can serve as spectral decomposition probes of spin bath dynamics, including the role of impurity inhomogeneity and hyperfine interactions between the ^{13}C and N spin baths.[32] In particular, such studies can provide substantial insight into the effects of environmental inhomogeneity for samples with high densities of NV centers and correspondingly high concentrations of N spin impurities. Such information cannot be extracted from single NV measurements, which require low NV densities to resolve individual NV centers optically.

III. MULTIPULSE MAGNETOMETRY

We next applied dynamical decoupling to improve the sensitivity of NV multispin magnetometry. In a standard ac magnetometry measurement utilizing a Hahn echo sequence, an oscillating magnetic field $b(t) = b_{\rm ac} \sin[(2\pi/\tau_{\rm ac})t + \phi]$ induces a net phase accumulation of the NV spin coherence, which is maximized when the full time of the Hahn echo sequence is equivalent to the period of the ac magnetic field ($\tau_{\rm ac}$) and the phase offset ϕ is such that the control pulses coincide with nodes in the magnetic field [Fig. 1(c)]. Under these conditions, the field amplitude $b_{\rm ac}$ can be extracted from the measurement of accumulated NV spin phase with optimum sensitivity normalized per unit time, given approximately by[1]

$$\eta_{\rm HE} \approx \frac{\pi\hbar}{2g\mu_B} \frac{1}{C\sqrt{\tau_{\rm ac}}} \exp\left[\left(\frac{\tau_{\rm ac}}{T_2}\right)^p\right]. \qquad (1)$$

Here C is a parameter that encompasses the measurement contrast, optical collection efficiency, and number of NV spins contributing to the measurement. The contrast is modified by NV decoherence over the course of the measurement, described phenomenologically by an exponential factor with power p. The value of p is found to be sample dependent, in the range of 1 to 2.5, and is related to the dynamics of the spin environment and to ensemble inhomogeneous broadening.[32]

In an ac magnetometry measurement utilizing n-pulse dynamical decoupling, the sensitivity is given approximately by Eq. (1) with two modifications: (1) the measurement time is increased by $\tau_{\rm ac} \to \frac{n}{2}\tau_{\rm ac}$, and (2) the NV multispin coherence time is extended by $T_2 \to T_2 n^s$. The resulting sensitivity is given by

$$\eta_{(n)} \approx \frac{\pi\hbar}{2g\mu_B} \frac{1}{C\sqrt{\frac{n}{2}\tau_{\rm ac}}} \exp\left[\left(\frac{n^{(1-s)}\tau_{\rm ac}}{2T_2}\right)^p\right]. \qquad (2)$$

Because the measurement time increases linearly with the number of control pulses n, whereas the coherence time increases sublinearly, there is an optimum number of pulses $n_{\rm opt}$ that yields the most sensitive measurement of an ac magnetic field of period $\tau_{\rm ac}$ given a set of sample-determined parameters:

$$n_{\rm opt} = \left[\frac{1}{2p(1-s)}\left(\frac{2T_2}{\tau_{\rm ac}}\right)^p\right]^{\frac{1}{p(1-s)}}. \qquad (3)$$

For a given sample, all the parameters except $\tau_{\rm ac}$ are fixed and we can simplify Eq. (3) to $n_{\rm opt} \propto (1/\tau_{\rm ac})^{\frac{1}{(1-s)}}$. From this relationship we see that at higher ac frequencies more pulses are needed to reach the optimum sensitivity, which can be understood intuitively by realizing that the high frequency regime corresponds to short time intervals between control pulses during which time there is very little contrast lost due to decoherence ($\tau_{\rm ac} \ll T_2$). More pulses increase the sensitivity by allowing for a longer measurement time and subsequently more phase accumulation per measurement. This intuition also illustrates why multipulse sequences are more effective at enhancing magnetometry sensitivity in the high-frequency regime, where the Hahn echo scheme provides relatively poor magnetic field sensitivity [Fig. 3(c)]. Note that extension of the NV multispin coherence time via multipulse dynamical decoupling (and thus enhancement of magnetic field sensitivity) is eventually limited by NV spin-lattice relaxation (T_1), beyond which increasing the number of control pulses is ineffective.

We used sample C to perform NV multispin magnetometry measurements comparing Hahn echo and multipulse dynamical decoupling schemes. The diamond detection volume was approximately 30 μm^3, corresponding to $\sim 10^3$ sensing NV centers aligned along the static magnetic field. We employed n-pulse XY sequences, in which control pulses are applied with the same timing as in CPMG-n sequences but with alternating 90° spin rotation axes to provide more isotropic compensation for pulse errors.[19] We note that such pulse sequences are equally applicable for samples with natural abundance of ^{13}C. Figure 3(a) illustrates how we extracted the magnetic field sensitivity from the measured variation of NV fluorescence as a function of applied ac magnetic field amplitude[1,2] for different

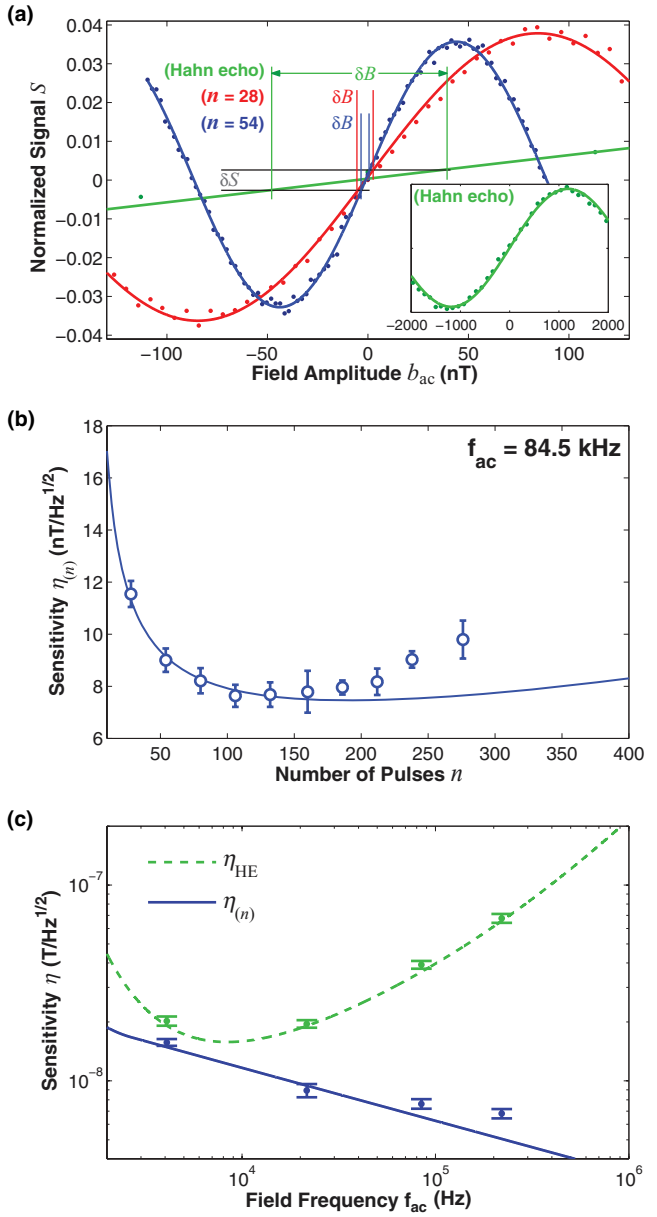

FIG. 3. (Color online) Measured ac magnetic field sensitivity for a 30 μm^3 sensing volume of sample C ($\sim 10^3$ sensing NV spins). (a) Examples of measured normalized fluorescence signals as functions of ac field magnitude b_{ac} using a Hahn echo sequence (green/light gray) (wider amplitude range shown in the inset) and multipulse XY sequences with 28 (red/gray) and 54 (blue/dark gray) control pulses, illustrating how the uncertainty in the measured signal (δS) limits the uncertainty in the extracted magnetic field magnitude (δB). The sine behavior of the signal with respect to b_{ac} is achieved by shifting the phase of the last microwave pulse by 90° from what is shown in Fig. 1(c). (b) Measured multipulse magnetic field sensitivity as a function of number of pulses for an 84.5 kHz ac field (circles). The solid line is calculated using Eq. (2) with experimental parameters $C = 0.1$, $T_2 = 250$ μs, $p = 1$, and $s = 0.37$. (c) Comparison of calculated (lines) and measured (points) magnetic field sensitivity at several ac field frequencies, for both Hahn echo and multipulse XY sequences (using the measured optimum number of pulses for each frequency).

measurement pulse sequences, normalized to measurement time (see Ref. 30 for details). The ac magnetic field sensitivity improved with the number of pulses, in good agreement with predicted values up to $n \approx 150$ pulses, at which point pulse infidelities began to degrade the measured sensitivity [Fig. 3(b)]. While for the present measurements the ac magnetic field consisted of a locked, single frequency component, the procedure can be easily extended to finite-bandwidth fields.[14]

Over a wide range of ac magnetic field frequencies our NV multispin measurements confirmed that multipulse dynamical decoupling outperformed the Hahn echo scheme, in agreement with theoretical expectations [Fig. 3(c)]. The enhancement in magnetic field sensitivity provided by multipulse dynamical decoupling was especially pronounced at frequencies higher than the Hahn echo $1/T_2$ coherence. For example, at a frequency of 220 kHz, we measured a factor of 10 improvement in magnetic field sensitivity from 67.7 ± 3.5 nT/$\sqrt{\text{Hz}}$ using a Hahn echo sequence, to 6.8 ± 0.4 nT/$\sqrt{\text{Hz}}$ using a 240-pulse XY sequence. Note that the present work demonstrates the efficacy of multipulse dynamical decoupling for NV multispin systems in samples with widely differing spin impurity environments, and the resulting relative improvement in magnetic field sensitivity. Ultimate performance of NV magnetometers will require optimization of many interrelated factors, including NV density and coherence time, spin impurity concentration, photon collection efficiency, signal contrast, etc.

IV. SUMMARY

In summary, we experimentally demonstrated that multipulse dynamical decoupling control sequences extend by an order of magnitude the coherence lifetime of large numbers ($>10^3$) of NV electronic spins in room temperature diamond for samples with widely differing NV densities and spin impurity environments. For these spin environments that differ from those studied previously, we found significantly different scaling of the NV multispin coherence time with the number of pulses in the control sequence. These results provide insight into spin-bath dynamics, and could guide future applications in multispin quantum information processing and metrology. We realized an extension of the NV multispin coherence time to >2 ms, which is comparable to the best results from application of dynamical decoupling to single NV centers. We also showed that multipulse dynamical decoupling improves NV multispin ac magnetic field sensitivity relative to the Hahn echo scheme, with a tenfold enhancement for higher frequency fields. Further improvements in NV multispin coherence time and magnetic field sensitivity are expected from the integration of dynamical decoupling with diamond samples engineered to have optimized spin environments. This work can be combined with parallel efforts such as implementing quantum-assisted techniques[33] and increased optical collection efficiency[24,34,35] and signal contrast[12] to realize an optimized NV ensemble magnetic field imager.[21] The present results also aid the development of scalable applications of quantum information and metrology in a variety of solid-state multispin systems, including NV centers in bulk diamond, 2D arrays, and nanostructures; phosphorous donors in silicon; and quantum dots.

ACKNOWLEDGMENTS

This work was supported by NIST, NSF, and DARPA (QuEST and QuASAR programs). We gratefully acknowledge the provision of diamond samples by Element Six and Apollo and helpful technical discussions with Daniel Twitchen and Matthew Markham.

[1] J. Taylor, P. Cappellaro, L. Childress, L. Jiang, D. Budker, P. R. Hemmer, A. Yacoby, R. Walsworth, and M. D. Lukin, Nat. Phys. **4**, 810 (2008).

[2] J. R. Maze, P. L. Stanwix, J. S. Hodges, S. Hong, J. M. Taylor, P. Cappellaro, L. Jiang, M. V. G. Dutt, E. Togan, A. S. Zibrov, A. Yacoby, R. L. Walsworth, and M. D. Lukin, Nature (London) **455**, 644 (2008).

[3] G. Balasubramanian, I. Y. Chan, R. Kolesov, M. Al-Hmoud, J. Tisler, C. Shin, C. Kim, A. Wojcik, P. R. Hemmer, A. Kreuger, T. Hanke, A. Leitenstorfer, R. Bratschitsch, F. Jelezko, and J. Wrachtrup, Nature (London) **455**, 648 (2008).

[4] C. L. Degen, Appl. Phys. Lett. **92**, 243111 (2008).

[5] G. Balasubramanian, P. Neumann, D. Twitchen, M. Markham, R. Kolesov, N. Mizuochi, J. Isoya, J. Achard, J. Beck, J. Tissler, V. Jacques, P. R. Hemmer, F. Jelezko, and J. Wrachtrup, Nat. Mater. **8**, 383 (2009).

[6] P. C. Maurer, J. R. Maze, P. L. Stanwix, L. Jiang, A. V. Gorshkov, A. A. Zibrov, B. Harke, J. S. Hodges, A. S. Zibrov, A. Yacoby, D. Twitchen, S. W. Hell, R. L. Walsworth, and M. D. Lukin, Nat. Phys. **6**, 912 (2010).

[7] M. S. Grinolds, P. Maletinsky, S. Hong, M. D. Lukin, R. L. Walsworth, and A. Yacoby, Nat. Phys. **7**, 687 (2011).

[8] F. Dolde, H. Fedder, M. W. Doherty, T. Noebauer, F. Rempp, G. Balasubramanian, T. Wolf, F. Reinhard, L. C. L. Hollenberg, F. Jelezko, and J. Wrachtrup, Nat. Phys. **7**, 459 (2011).

[9] P. Maletinsky, S. Hong, M. S. Grinolds, B. Hausmann, M. D. Lukin, R. L. Walsworth, M. Loncar, and A. Yacoby, Nat. Nanotechnol. **7**, 320 (2012).

[10] V. M. Acosta, E. Bauch, A. Jarmola, L. J. Zipp, M. P. Ledbetter, and D. Budker, Appl. Phys. Lett. **97**, 174104 (2010).

[11] C. S. Shin, C. E. Avalos, M. C. Butler, D. R. Trease, S. J. Seltzer, J. P. Mustonen, D. J. Kennedy, V. M. Acosta, D. Budker, A. Pines, and V. S. Bajaj, arXiv:1201.3152v1.

[12] L. M. Pham, N. Bar-Gill, D. Le Sage, A. Stacey, M. Markham, D. J. Twitchen, M. D. Lukin, and R. L. Walsworth (2012) arXiv:1207.3363.

[13] G. de Lange, Z. H. Wang, D. Riste, V. V. Dobrovitski, and R. Hanson, Science **330**, 60 (2010).

[14] G. de Lange, D. Riste, V. V. Dobrovitski, and R. Hanson, Phys. Rev. Lett. **106** 080802 (2011).

[15] C. A. Ryan, J. S. Hodges, and D. G. Cory, Phys. Rev. Lett. **105** 200402 (2010).

[16] B. Naydenov, F. Dolde, L. T. Hall, C. Shin, H. Fedder, L. C. L. Hollenberg, F. Jelezko, and J. Wrachtrup, Phys. Rev. B **83** 081201 (2011).

[17] H. Y. Carr and E. M. Purcell, Phys. Rev. **94**, 630 (1954).

[18] S. Meiboom and D. Gill, Rev. Sci. Instrum. **29**, 688 (1958).

[19] T. Gullion, D. B. Baker, and M. S. Conradi, J. Magn. Reson. **89**, 479 (1990).

[20] P. L. Stanwix, L. M. Pham, J. R. Maze, D. Le Sage, T. K. Yeung, P. Cappellaro, P. R. Hemmer, A. Yacoby, M. D. Lukin, and R. L. Walsworth, Phys. Rev. B **82**, 201201 (2010).

[21] L. M. Pham, D. Le Sage, P. L. Stanwix, T. K. Yeung, D. Glenn, A. Trifonov, P. Cappellaro, P. R. Hemmer, M. D. Lukin, H. Park, A. Yacoby, and R. L. Walsworth, New J. Phys. **13**, 045021 (2010).

[22] S. Steinert, F. Dolde, P. Neumann, A. Aird, B. Naydenov, G. Balasubramanian, F. Jelezko, and J. Wrachtrup, Rev. Sci. Instrum. **81**, 043705 (2010).

[23] B. J. Maertz, A. P. Wijnheijmer, G. D. Fuchs, M. E. Nowakowski, and D. D. Awschalom, Appl. Phys. Lett. **96**, 092504 (2010).

[24] T. M. Babinec, B. J. M. Hausmann, M. Khan, Y. Zhang, J. R. Maze, P. R. Hemmer, and M. Loncar, Nat. Nanotech. **5**, 195 (2010).

[25] P. G. Baranov, A. A. Soltamova, D. O. Tolmachev, N. G. Romanov, R. A. Babunts, F. M. Shakhov, S. V. Kidalov, A. Y. Vul', G. V. Mamin, S. B. Orlinskii, and N. I. Silkin, Small **7**, 1533 (2011).

[26] A. M. Tyryshkin, S. A. Lyon, A. V. Astashkin, and A. M. Raitsimring, Phys. Rev. B **68**, 193207 (2003).

[27] S. Simmons, R. M. Brown, H. Riemann, N. V. Abrosimov, P. Becker, H.-J. Pohl, M. L. W. Thewalt, K. M. Itoh, and J. J. L. Morton, Nature (London) **470**, 69 (2011).

[28] R. Hanson, L. P. Kouwenhoven, J. R. Petta, S. Tarucha, and L. M. K. Vandersypen, Rev. Mod. Phys. **79**, 1217 (2007).

[29] L. Childress, M. V. G. Dutt, J. M. Taylor, A. S. Zibrov, F. Jelezko, J. Wrachtrup, P. R. Hemmer, and M. D. Lukin, Science **314**, 281 (2006).

[30] See Supplemental Material at http://link.aps.org/supplemental/10.1103/PhysRevB.86.045214 for additional technical details and experimental analysis.

[31] C. P. Slichter, *Principles of Magnetic Resonance* (Springer,Berlin, 1990).

[32] N. Bar-Gill, L. M. Pham, C. Belthangady, D. Le Sage, P. Cappellaro, J. R. Maze, M. D. Lukin, A. Yacoby, and R. L. Walsworth, Nat. Commun. **3**, 858 (2012).

[33] L. Jiang, J. S. Hodges, J. R. Maze, P. Maurer, J. M. Taylor, D. G. Cory, P. R. Hemmer, R. L. Walsworth, A. Yacoby, A. S. Zibrov, and M. D. Lukin, Science **326**, 267 (2009).

[34] D. Le Sage, L. M. Pham, N. Bar-Gill, C. Belthangady, M. D. Lukin, A. Yacoby, and R. L. Walsworth, Phys. Rev. B **85**, 121202(R) (2012).

[35] T. K. Yeung, D. Le Sage, L. M. Pham, P. L. Stanwix, and R. L. Walsworth, Appl. Phys. Lett. **100**, 251111 (2012).